TGFβ-mediated dural progenitor cell migration into the coronal suture is crucial for preventing craniosynostosis

This document includes:

Supplementary Fig. 1 to Supplementary Fig. 13

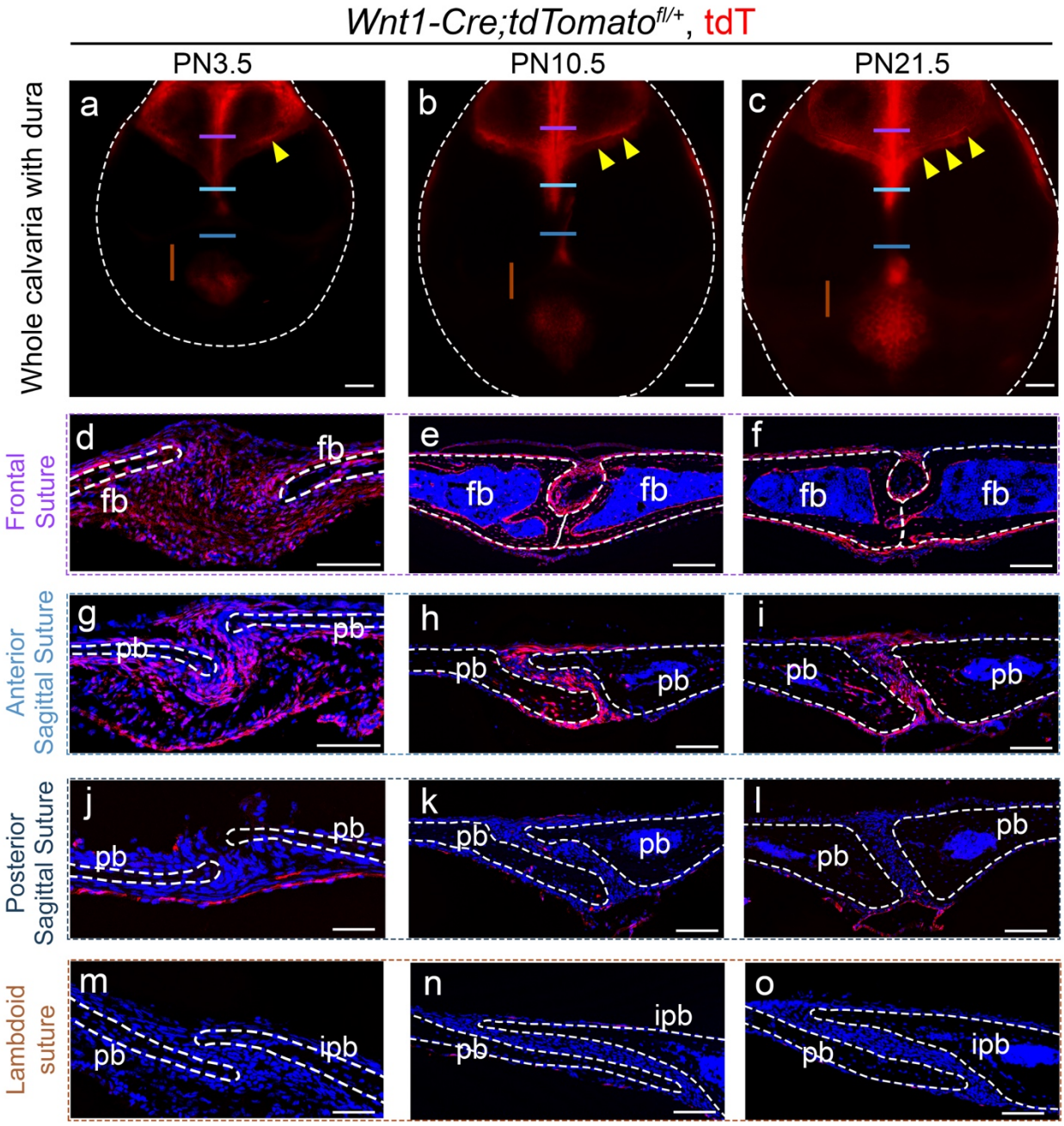

Supplementary Fig. 1: Contribution of CNC-derived cells to cranial sutures.

(a-c) Whole-mount fluorescence images showing tdT+ (red) cells in the *Wnt1-Cre;tdTomato*$^{fl/+}$ calvaria at PN3.5 (a), PN10.5 (b), and PN21.5 (c). Arrowheads indicate the presence of tdT+ cells

in the suture. Purple, light blue, dark blue, and brown lines indicate the planes of sections shown in (d-f), (g-i), (j-l), and (m-o), respectively.

(d-o) Fluorescence images of tdT+ cells in different *Wnt1-Cre;tdTomato*$^{fl/+}$ suture sections at the indicated stages. (d-f) The frontal suture mesenchyme and its underlying dura at PN3.5 (d), PN10.5 (e), and PN21.5 (f). (g-i) The anterior sagittal suture mesenchyme and its underlying dura at PN3.5 (g), PN10.5 (h), and PN21.5 (i). (j-l) The posterior sagittal suture mesenchyme and its underlying dura at PN3.5 (j), PN10.5 (k), and PN21.5 (l). (m-o) The lambdoid suture mesenchyme and its underlying dura at PN3.5 (m), PN10.5 (n), and PN21.5 (o).

Scale bars: 1 mm in (a-c); 100 μm in (d-o).

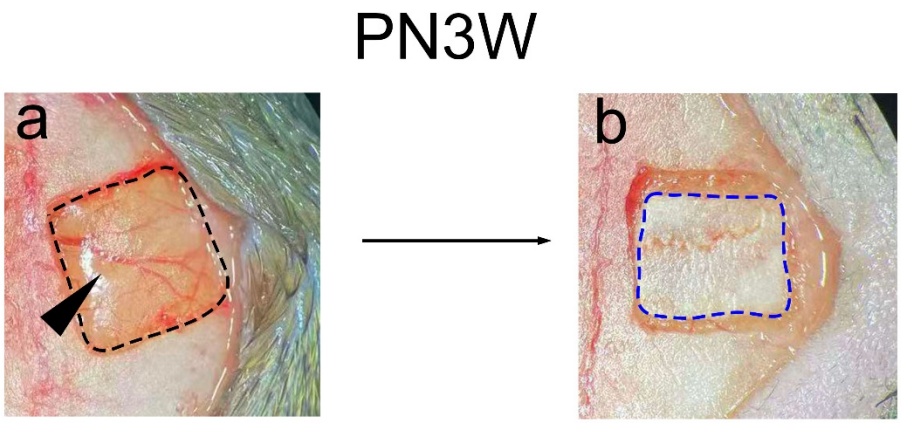

Supplementary Fig. 2: Suture transplantation surgery procedure.

(a) Exposure of the PN3W dura for suture transplantation. The cranial suture region of PN3W recipient mice was exposed by carefully removing the overlying calvarial bone. The underlying dura remained intact and served as the recipient surface for transplants. The black dashed lines and arrowhead indicate the exposed dura after the calvarial bone was removed. (b) Transplantation of PN3.5 donor suture region onto PN3W dura. The PN3.5 cranial suture, together with adjacent cranial bone segments, was placed onto the exposed dura mater of PN3W recipient mice at the corresponding anatomical location. The graft was aligned along the anterior-posterior axis of the suture to ensure proper orientation. The blue dashed line outlines the PN3.5 donor suture region in its transplanted location.

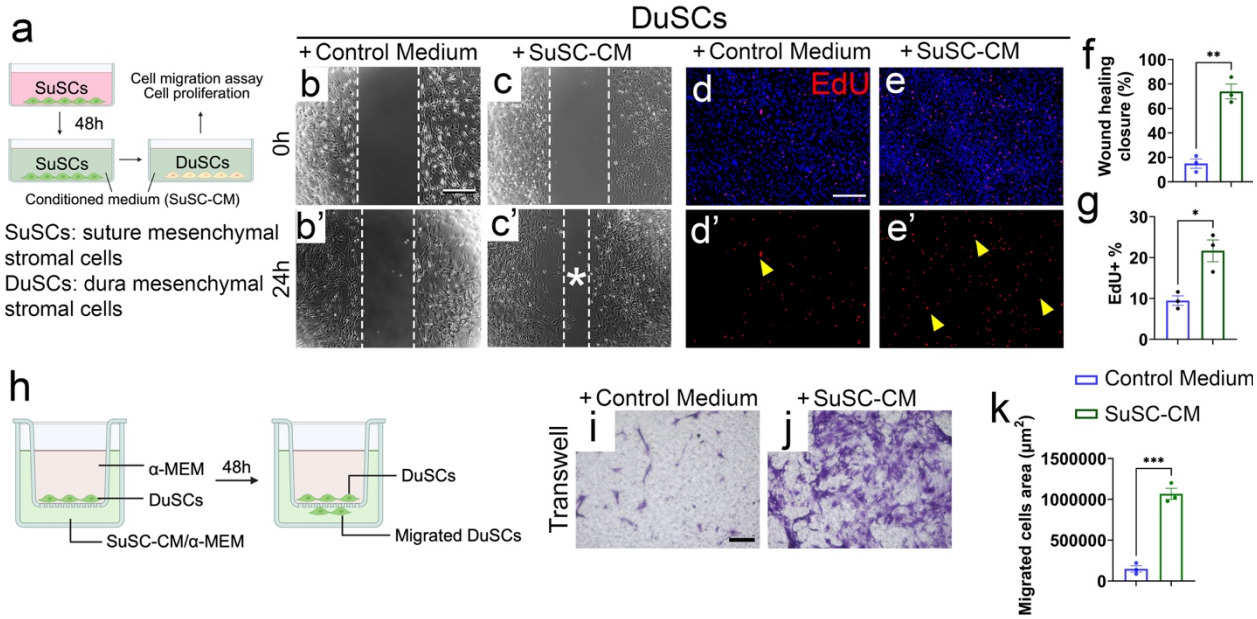

Supplementary Fig. 3: Suture mesenchymal stromal cells (SuSCs) promote dural cell proliferation and migration.

(a) Diagram showing the procedure of SuSC-conditioned medium (SuSC-CM) transfer to DuSCs, followed by downstream assays. SuSCs were cultured for 48 h to produce SuSC-CM, which was collected and applied to DuSCs for migration and proliferation assays. Created in BioRender. Feng, J. (2026) https://BioRender.com/ybqp718.

(b-c) Cell migration assays showing wound healing ability of DuSCs treated with control medium (b-b') and SuSC-CM (c-c'). Migration distance is indicated by the two white dashed lines marking the leading edges of DuSCs. Asterisks indicate impaired cell migration.

(d-e) EdU staining (red) of the cultured DuSCs treated with control medium and SuSC-CM. Yellow arrowheads indicate EdU+ cells.

(f) Quantitative data in (b, c) are presented as mean ± SEM, $p = 0.0012$, **, calculated by two-tailed unpaired t-test, N = 3.

(g) Quantitative data in (d, e) are presented as mean ± SEM, $p = 0.0141$, *, calculated by two-tailed unpaired t-test, N = 3.

(h) Diagram showing procedures of the transwell assay in (i, j). Created in BioRender. Feng, J. (2026) https://BioRender.com/w6xj683.

(i, j) Transwell assays showing migration ability of DuSCs when treated with control medium (i) and SuSC-CM (j). Blue staining shows cells.

(k) Quantitative data in (i, j) are presented as mean ± SEM, $p = 0.0003$, ***, calculated by two-tailed unpaired t-test, N = 3.

Scale bars: 200 μm in b (b, c, b', c'), d (d, e, d', e'), and i (i, j). Source data are provided as a Source Data file.

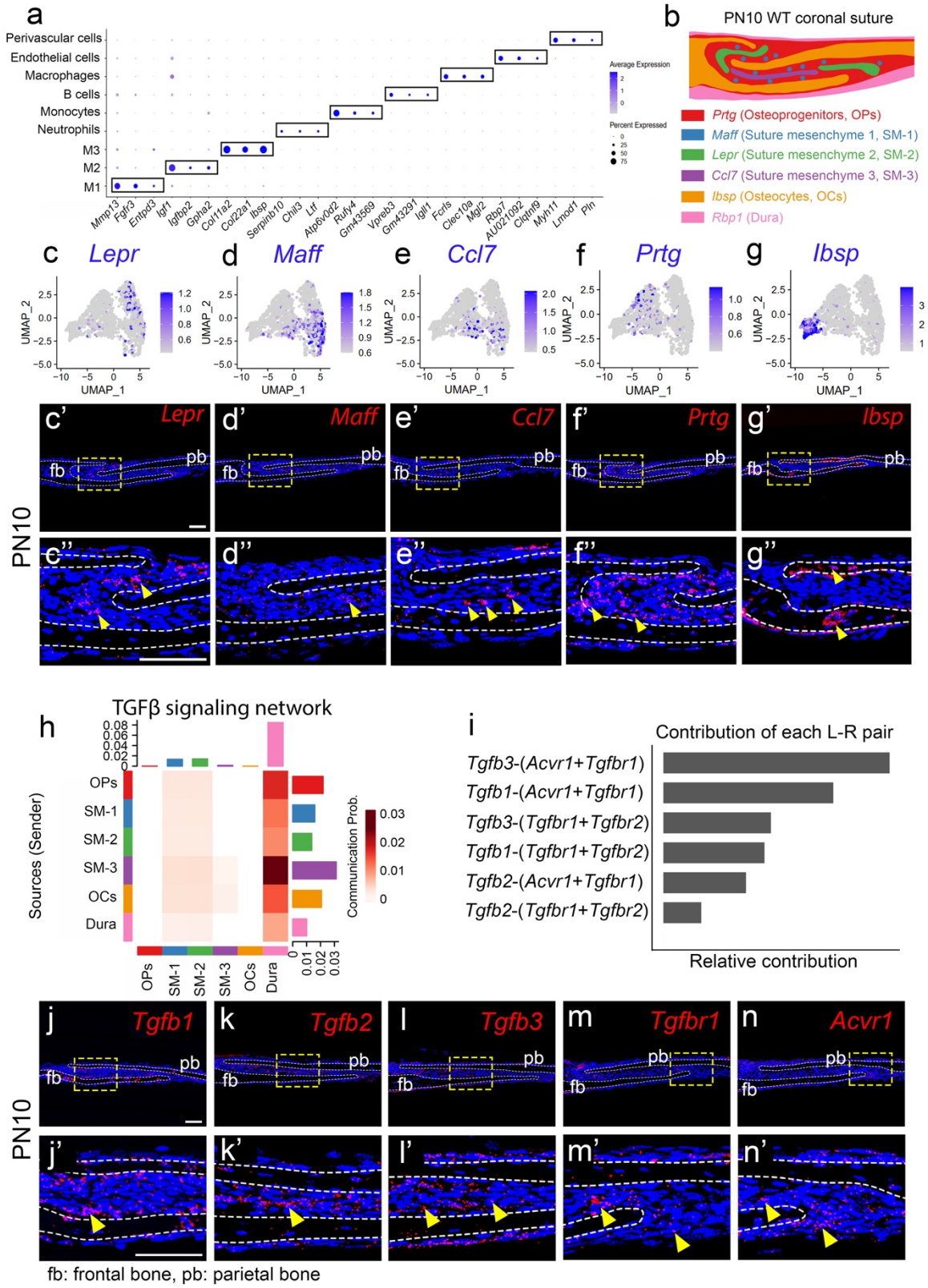

fb: frontal bone, pb: parietal bone

Supplementary Fig. 4: scRNA-seq analysis reveals the TGFβ signaling pathway as an important mediator of coronal suture-to-dura signaling.

(a) Dotplot showing the top three differentially expressed marker genes (boxed) for each population.

(b) Schematic summarizing the spatial distribution of suture mesenchymal populations.

(c-g) Feature plots and RNAscope staining of markers for suture mesenchymal populations. (c''-g'') are magnified views of the yellow boxed areas in (c'-g'), respectively. Dashed outlines indicate the frontal bone (fb) and parietal bone (pb). Arrowheads indicate positive signals.

(h) Cell-cell communication analysis of TGFβ signaling in the suture mesenchyme to dura interaction.

(i) Ligand-receptor analysis showing the possible paired ligands and receptors of the TGFβ signaling pathway involved in the suture mesenchyme to dura interaction.

(j-n) RNAscope staining showing the expression patterns of TGFβ signaling ligands (red): *Tgfb1-Tgfb3* (j-l) and receptors (red): *Tgfbr1* (m) and *Acvr1* (n). (j'-n') are magnified views of the yellow boxed areas in (j-n), respectively. Dashed outlines indicate the frontal bone (fb) and parietal bone (pb). Arrowheads indicate positive signals.

Scale bars: 50 μm in c' (c'-g'), c'' (c''-g''), j (j-n), and j' (j'-n').

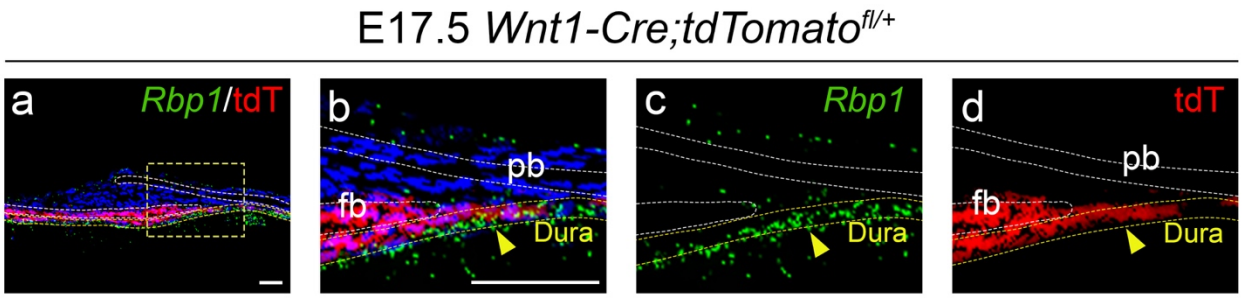

*fb: frontal bone; pb: parietal bone

Supplementary Fig. 5: *Rbp1* marks the dura and colocalizes with CNC-derived cells.

(a-d) RNAscope staining of *Rbp1* (green) and immunofluorescence staining of tdT (red) in the E17.5 *Wnt1-Cre;tdTomato*$^{fl/+}$ coronal suture region. Yellow arrowheads indicate colocalization of *Rbp1* and tdT. Boxed regions in (a) are shown at higher magnification in (b-d). fb, frontal bone; pb, parietal bone. Scale bars: 100 μm in a (a, c) and b (b, d).

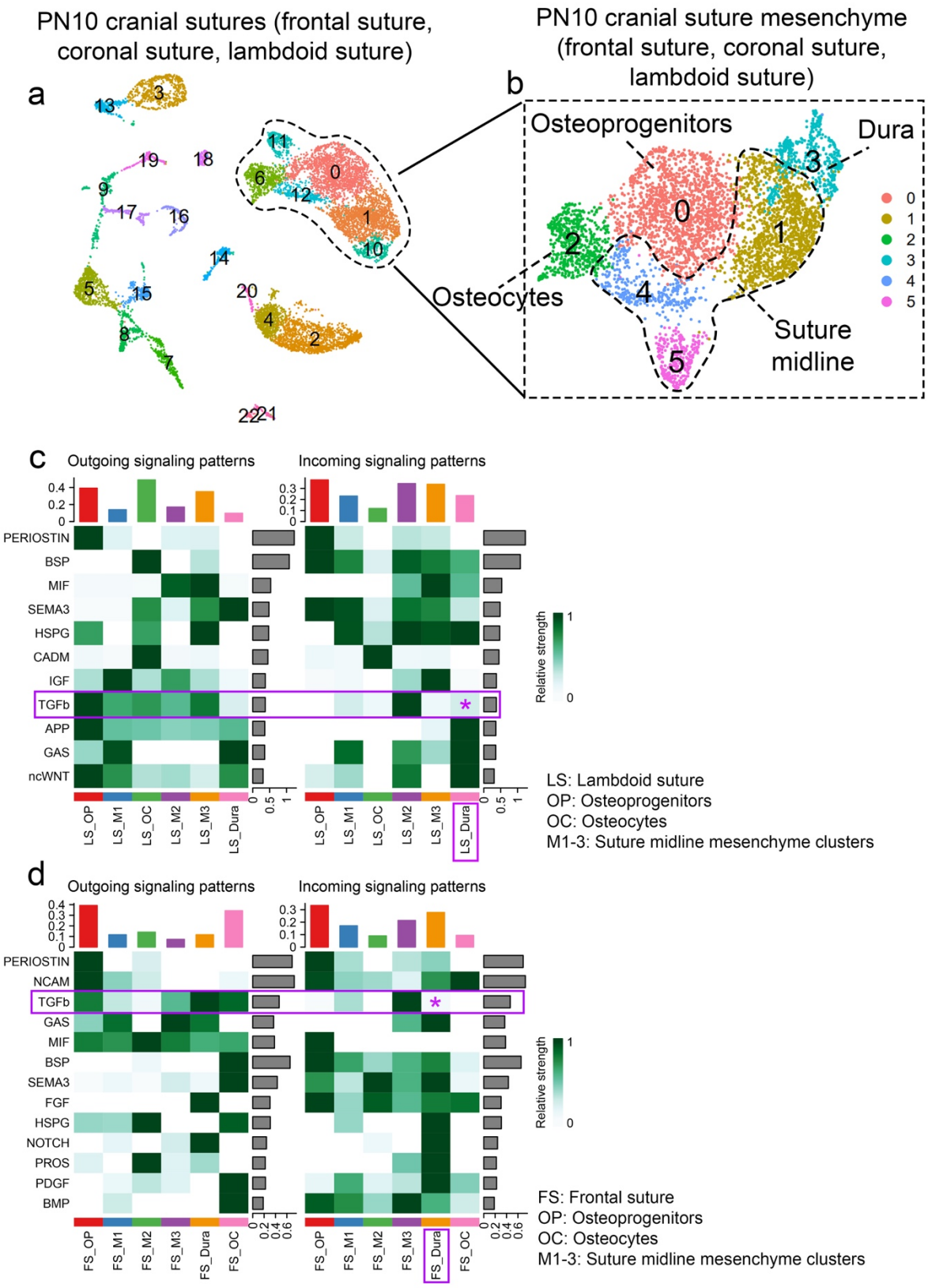
PN10 cranial sutures (frontal suture, coronal suture, lambdoid suture)
a
PN10 cranial suture mesenchyme (frontal suture, coronal suture, lambdoid suture)
b
Osteoprogenitors
Dura
Osteocytes
Suture midline
c
Outgoing signaling patterns
Incoming signaling patterns
PERIOSTIN
BSP
MIF
SEMA3
HSPG
CADM
IGF
TGFb
APP
GAS
ncWNT
Relative strength
LS_OP
LS_M1
LS_OC
LS_M2
LS_M3
LS_Dura
LS: Lambdoid suture
OP: Osteoprogenitors
OC: Osteocytes
M1-3: Suture midline mesenchyme clusters
d
Outgoing signaling patterns
Incoming signaling patterns
PERIOSTIN
NCAM
TGFb
GAS
MIF
BSP
SEMA3
FGF
HSPG
NOTCH
PROS
PDGF
BMP
Relative strength
FS_OP
FS_M1
FS_M2
FS_M3
FS_Dura
FS_OC
FS: Frontal suture
OP: Osteoprogenitors
OC: Osteocytes
M1-3: Suture midline mesenchyme clusters

84

Supplementary Fig. 6: TGFβ signaling is not present in the frontal or lambdoid suture-dura interaction.

(a) UMAP plot of integrated scRNA-seq datasets from PN10 WT sutures (frontal, coronal, and lambdoid). Dashed line indicates sutural mesenchymal populations.

(b) UMAP plot of the reclustered sutural mesenchymal populations subsetted from (a).

(c-d) CellChat analysis showing outgoing and incoming signaling patterns of mesenchymal cell populations in lambdoid (c) and frontal (d) suture regions. Asterisks indicate the absence of TGFβ signaling activity**.**

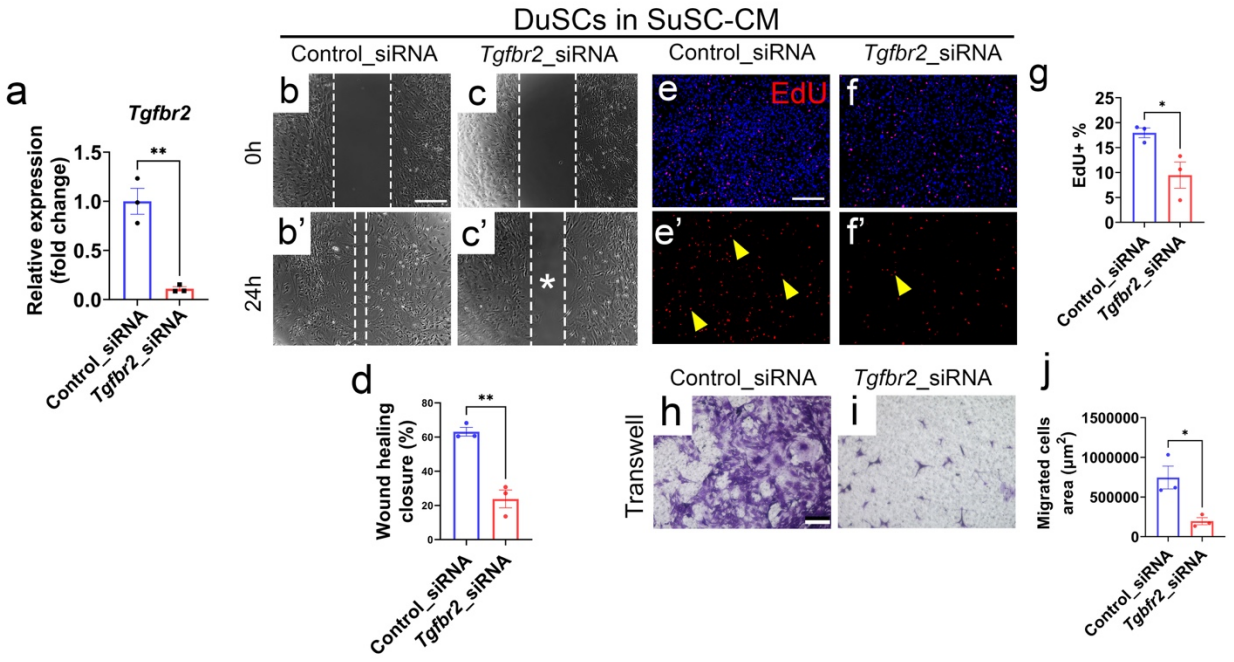

Supplementary Fig. 7: Suture mesenchymal stromal cells (SuSCs) promote dural cell proliferation and migration through the TGFβ signaling pathway.

(a) qPCR results of dural *Tgfbr2* levels following control_siRNA and *Tgfbr2*_siRNA treatment, $p = 0.0026$, **, two-tailed unpaired t-test, N = 3.

(b-c) Cell migration assay showing DuSC migration in the control_siRNA and *Tgfbr2*_siRNA treatment groups upon exposure to SuSC-CM. Migration distance is indicated by the two dashed lines marking the leading edge of DuSCs. Asterisks indicate impaired cell migration.

(d) Quantitative data in (b-c) are presented as mean ± SEM, $p = 0.0025$, **, N = 3, calculated by two-tailed unpaired t-test.

(e-f) EdU staining in cultured DuSCs exposed to SuSC-CM after treatment with control_siRNA and *Tgfbr2*_siRNA. Yellow arrowheads indicate EdU+ cells.

(g) Quantitative data in (e-f) are presented as mean ± SEM, p = 0.0385, *, N = 3, two-tailed unpaired t-test.

(h, i) Transwell assays showing migration ability following control_siRNA and *Tgfbr2*_siRNA treatment. Blue staining shows cells.

(j) Quantitative data in (h, i) are presented as mean ± SEM, p = 0.0217, *, N = 3, two-tailed unpaired t-test.

Scale bars: 200 μm in b (b, c, b', c'), e (e, f, e', f'), and h (h, i). Source data are provided as a Source Data file.

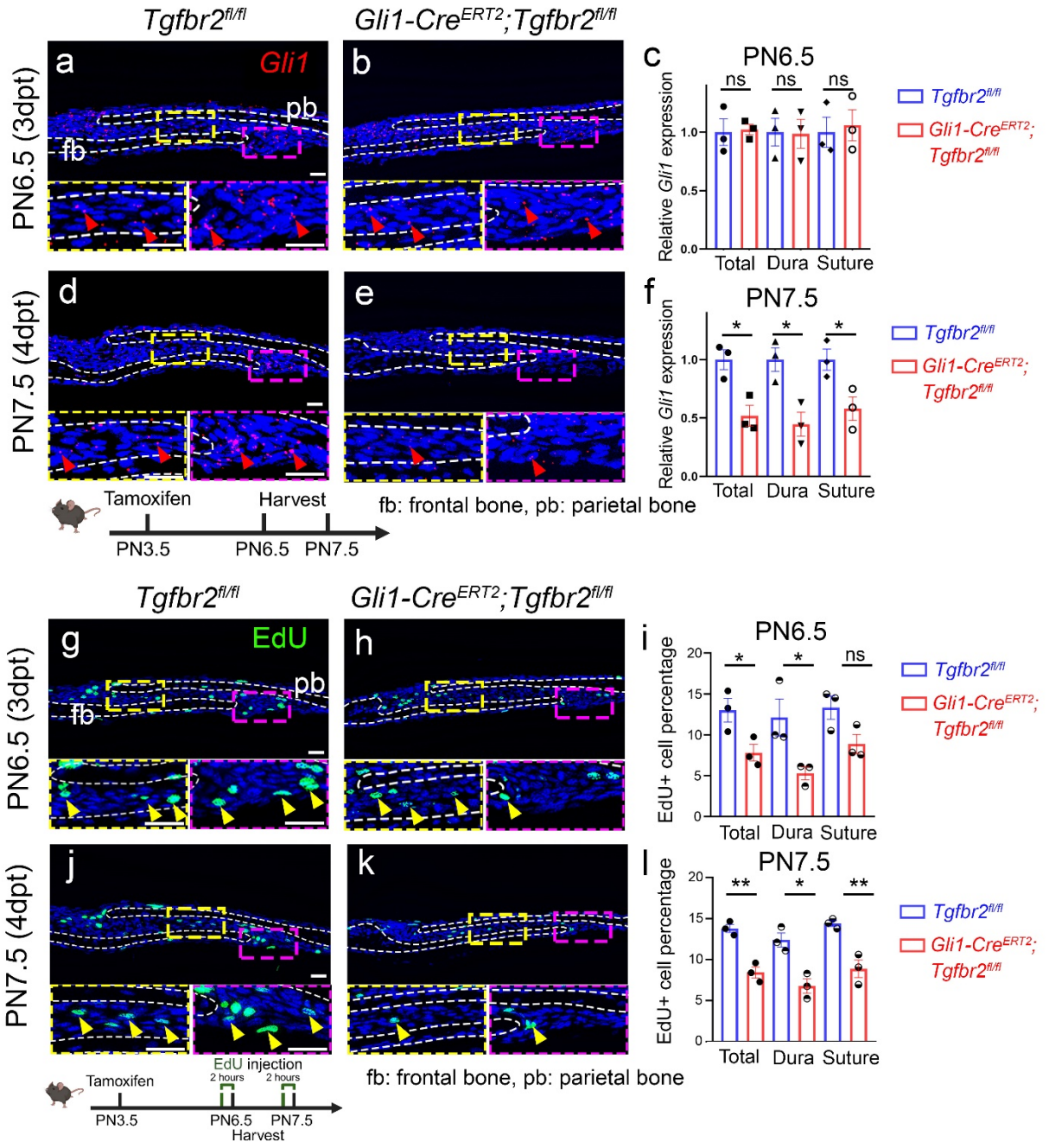

Supplementary Fig. 8: Loss of *Tgfbr2* in *Gli1*+ cells reduces dural cell proliferation and impairs suture homeostasis.

(a-f) RNAscope staining of *Gli1* in the coronal sutures of control and *Gli1-Cre^{ERT2};Tgfbr2$^{fl/fl}$* mice 3 and 4 days after tamoxifen induction. The yellow and purple boxed areas indicate the suture and

dura regions, respectively. Red arrowheads indicate *Gli1* expression. (c) Quantitative data in (a, b) are presented as mean ± SEM, two-tailed unpaired t-test, $p = 0.3560$, ns (Total), 0.9394, ns (Dura), 0.7626, ns (Suture), N = 3. (f) Quantitative data in (d, e) are presented as mean ± SEM, two-tailed unpaired t-test, $p = 0.0171$, * (Total), 0.0185, * (Dura), 0.0361, * (Suture), N = 3.

(g-l) Fluorescence images of EdU+ cells in the $Tgfbr2^{fl/fl}$ and $Gli1\text{-}Cre^{ERT2};Tgfbr2^{fl/fl}$ mice at 3 and 4 days after tamoxifen induction. The yellow and purple boxed areas indicate the suture and dura regions. Yellow arrowheads indicate EdU+ cells. (i) Quantitative data in (g-h) are presented as mean ± SEM, two-tailed unpaired t-test, $p = 0.0240$, * (Total), 0.0466, * (Dura), 0.0732, ns (Suture), N = 3. (l) Quantitative data in (j-k) are presented as mean ± SEM, two-tailed unpaired t-test, $p = 0.0028$, ** (Total), 0.0101, * (Dura), 0.0079, ** (Suture), N = 3.

Scale bars: 50 μm in a (a, b), d (d, e), g (g, h), j (j, k). Schematic illustration was created in BioRender. Feng, J. (2026) https://BioRender.com/siu6vm9. Source data are provided as a Source Data file.

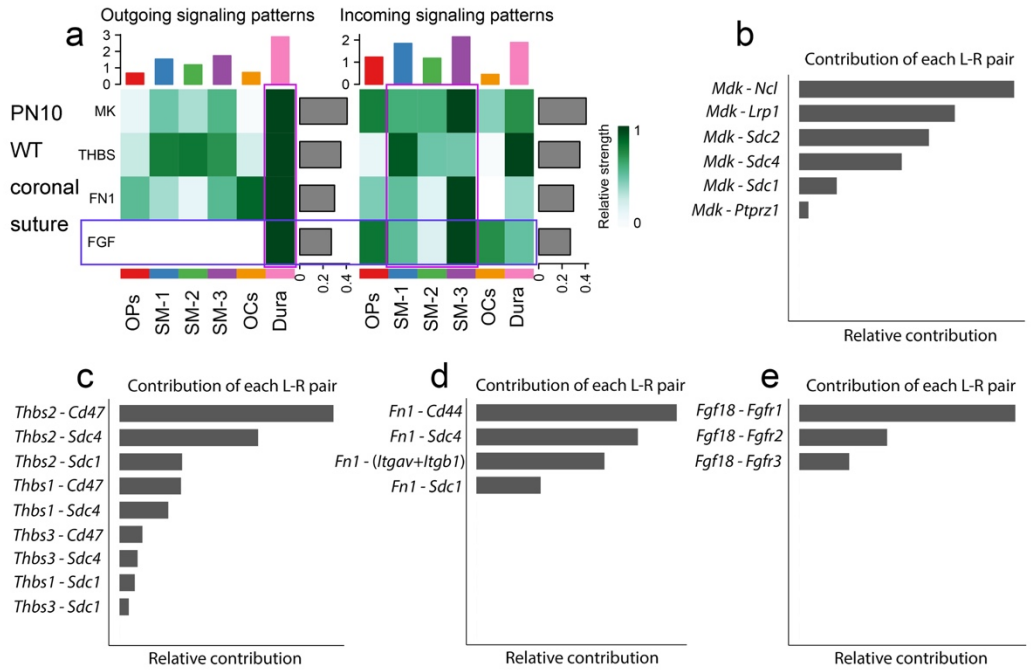

PN10 mouse coronal suture mesenchyme

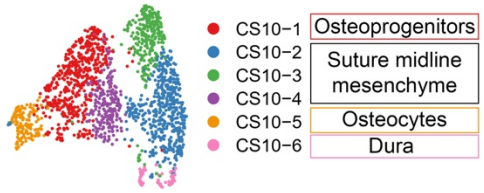

f Ligands

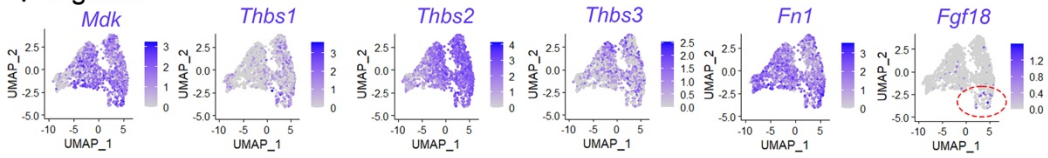

g Receptors

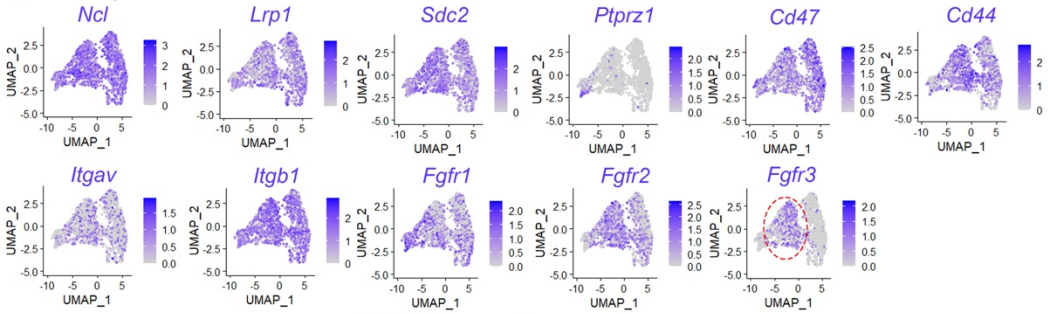

PN10 Control coronal suture

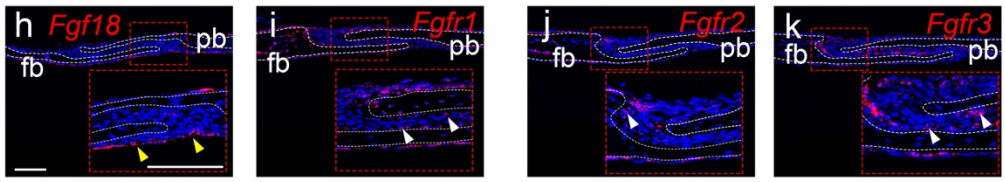

*fb: frontal bone; pb: parietal bone

134

Supplementary Fig. 9: CellChat analysis of other signaling pathways in dura-to-suture regulation.

(a) CellChat analysis of outgoing (left) and incoming (right) signaling patterns for different cell populations in the PN10 WT coronal suture region. Color intensity indicates relative signaling strength.

(b-e) Bar plots showing the relative contributions of individual ligand-receptor (L-R) pairs in the MK (b), THBS (c), FN1 (d), and FGF (e) signaling pathways.

(f) UMAP plots showing the expression patterns of selected ligands (*Mdk*, *Thbs1*, *Thbs2*, *Thbs3*, *Fn1*, *Fgf18*) of the identified signaling pathways across cell populations in the PN10 coronal suture region.

(g) UMAP plots showing the expression of corresponding receptors (*Ncl*, *Lrp1*, *Sdc2*, *Ptprz1*, *Cd47*, *Cd44*, *Itgav*, *Itgb1*, *Fgfr1*, *Fgfr2*, *Fgfr3*).

(h-k) RNAscope staining showing the *in vivo* expression of *Fgf18* (h), *Fgfr1* (i), *Fgfr2* (j), and *Fgfr3* (k) in the PN10 coronal suture. Red dashed boxes highlight regions of enrichment. Dotted lines outline the suture mesenchyme.

Scale bar: 100 μm in h (h-k).

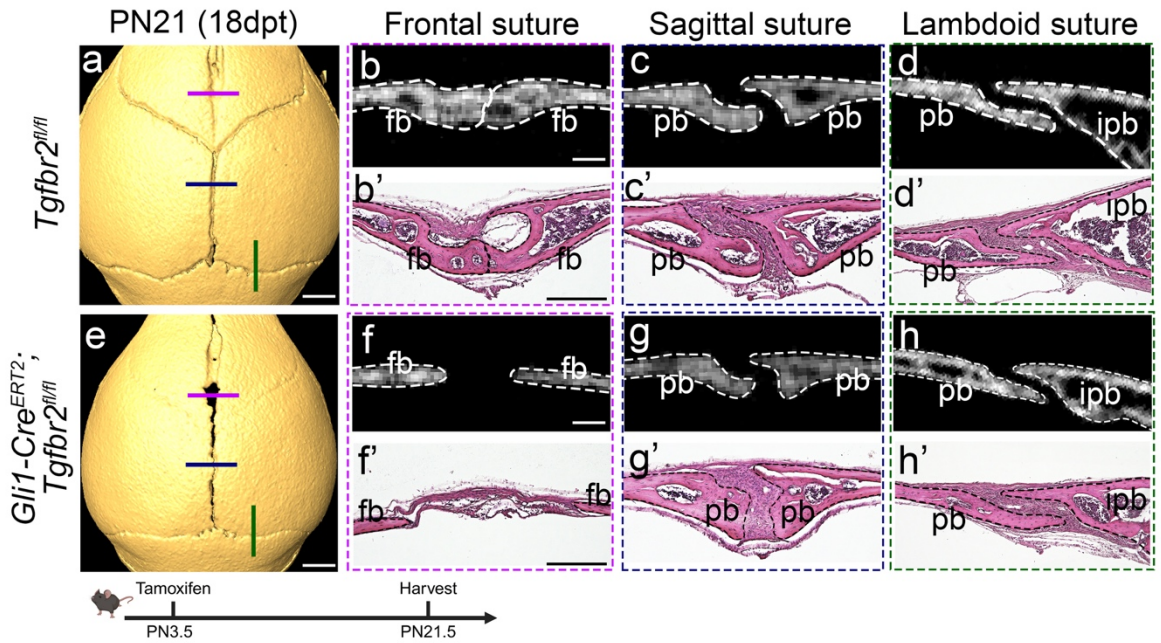

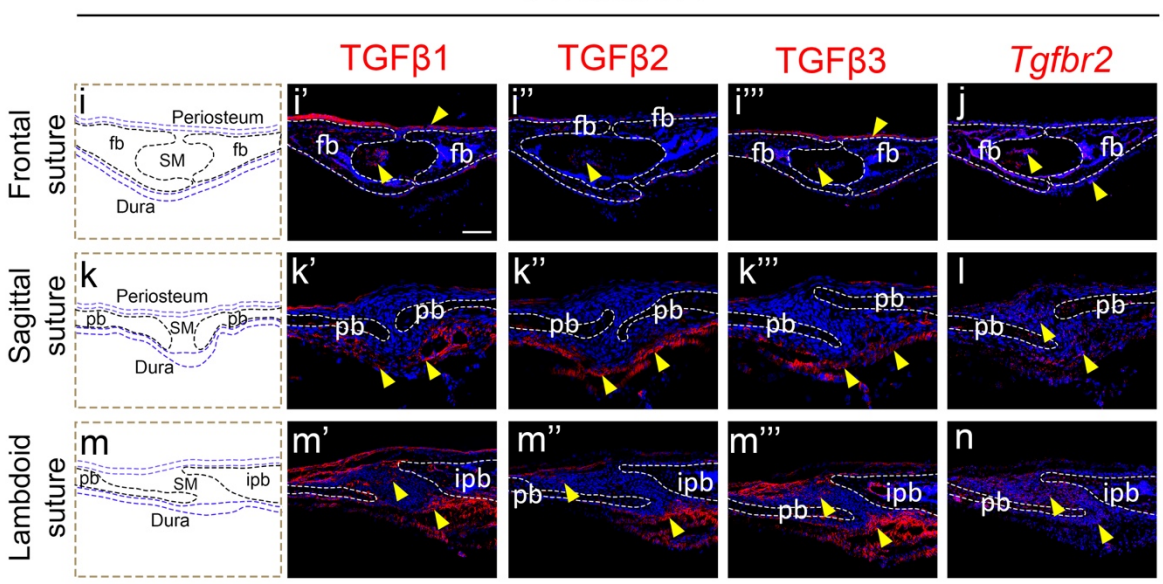

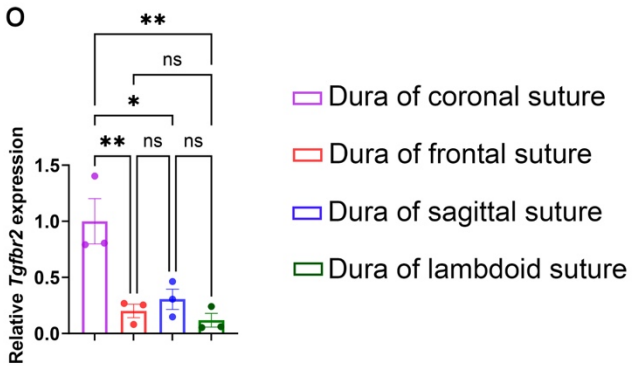

*fb: frontal bone; pb: parietal bone, ipb: interparietal bone

Supplementary Fig. 10: Loss of *Tgfbr2* in *Gli1*+ progenitor cells does not lead to frontal, sagittal, or lambdoid suture fusion.

(a-h) Micro-CT and H&E images showing the frontal suture (b, b', f, f'), sagittal suture (c, c', g, g'), and lambdoid suture (d, d', h, h') in $Tgfbr2^{fl/fl}$ and $Gli1\text{-}Cre^{ERT2};Tgfbr2^{fl/fl}$ mice.

(i-n) Expression patterns of TGFβ ligands and *Tgfbr2* in different cranial sutures at PN10.5. (i, k, m) Schematic illustrations of the frontal, sagittal, and lambdoid sutures, respectively, indicate periosteum, suture mesenchyme (SM), underlying dura, and adjacent bones. fb: frontal bone; pb: parietal bone; ipb: interparietal bone. (i'-j) Immunofluorescence staining of TGFβ1, TGFβ2, and TGFβ3 and RNAscope staining of *Tgfbr2* in the frontal suture at PN10.5. (k'-l) Corresponding staining in the sagittal suture. (m'-n) Corresponding staining in the lambdoid suture. White dashed lines outline the bone edges. Yellow arrowheads indicate regions with positive signals.

(o) Quantitative data in (j, l, n) are presented as mean ± SEM, calculated by one-way ANOVA with multiple comparisons, showing higher expression in coronal versus frontal (p = 0.0061), sagittal (p = 0.0137), and lambdoid sutures (p = 0.0034), with no differences among frontal, sagittal, and lambdoid groups (p = 0.9216, 0.9580, and 0.6892).

Scale bars: 1 mm in (a, e); 200 μm in b (b-d), b' (b'-d'), f (f-h), and f' (f'-h'); 100 μm in i' (i'-j, k'-l, m'-n). Schematic illustration was created in BioRender. Feng, J. (2026) https://BioRender.com/siu6vm9. Source data are provided as a Source Data file.

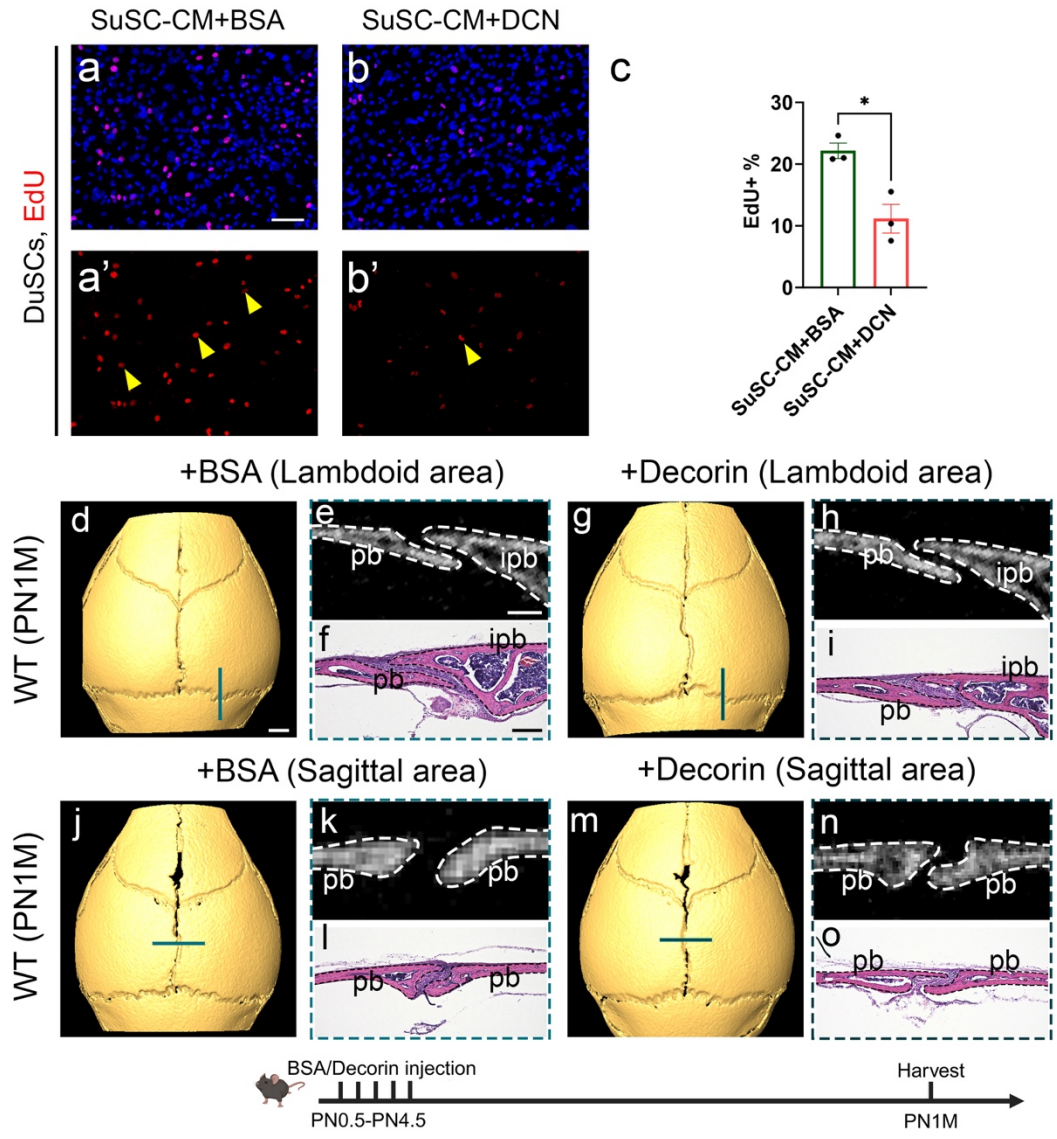

170

171 **Supplementary Fig. 11: The function of decorin in coronal dural cells, lambdoid suture, and**

172 **sagittal suture.**

173 (a-b) EdU (red) incorporation assays of DuSCs cultured with SuSC-CM supplemented with BSA

174 (control; a, a') or recombinant decorin (DCN; b, b').

175 (c) Quantitative data in (a-b) are presented as mean ± SEM, calculated by two-tailed unpaired t-

176 test, $p = 0.0141$, *, N = 3.

(d-o) Micro-CT 3D reconstructions, micro-CT slice images, and corresponding histological sections of WT mouse skulls following postnatal injection of BSA or decorin protein into lambdoid or sagittal suture regions. Decorin or BSA was injected daily from PN0.5 to PN4.5, and skulls were harvested at PN1M. Blue lines in d, g, j, and m indicate the section locations of (e, f), (h, i), (k, l) and (n, o), respectively. N = 3 per group. pb: parietal bone, ipb: interparietal bone.

Scale bars: 100 μm in a (a, b, a', b'); 1 mm in d (d, g, j, m); 200 μm in e (e, h, k, n) and f (f, i, l, o). Schematic illustration was created in BioRender. Feng, J. (2026) https://BioRender.com/siu6vm9.

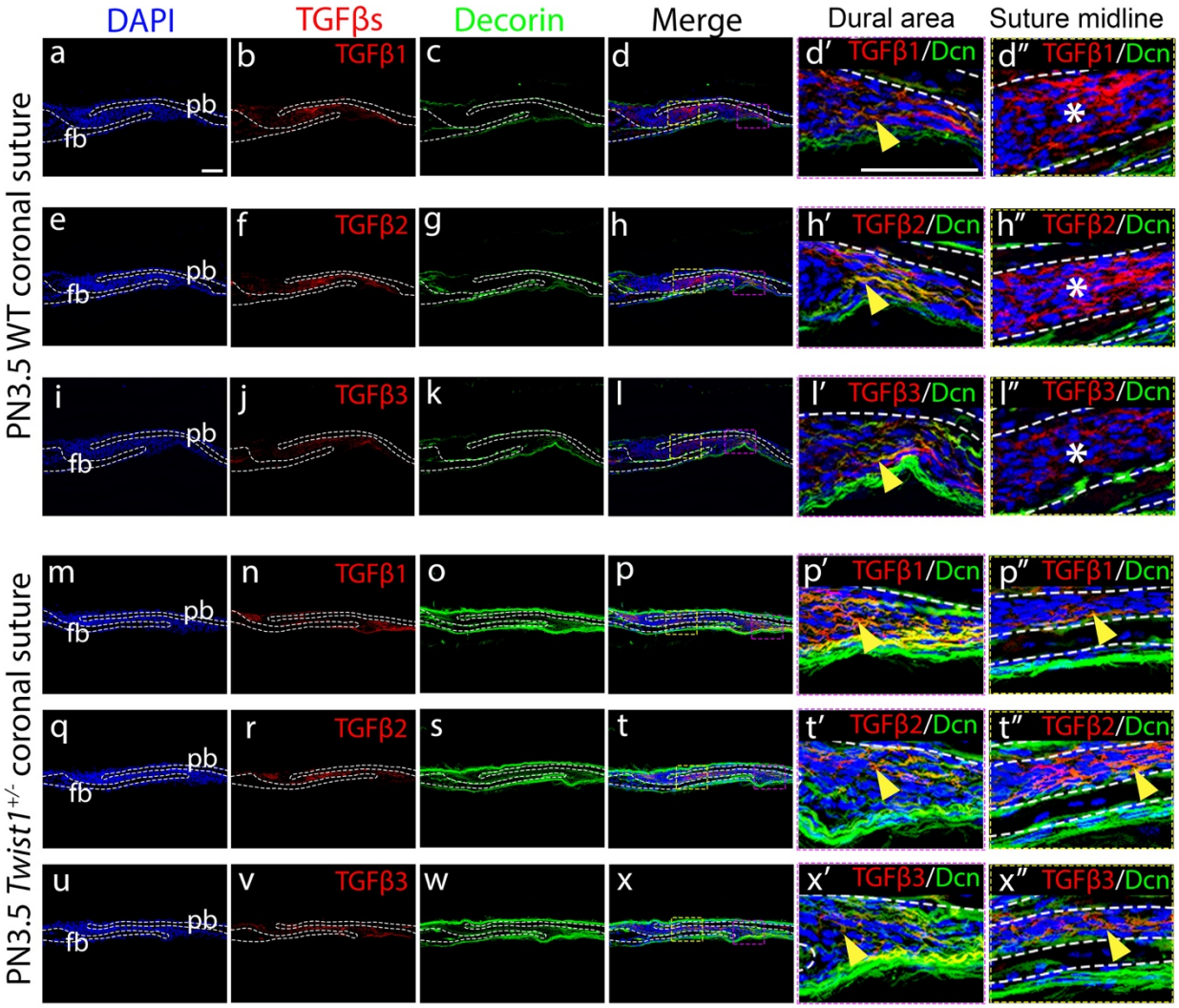

Supplementary Fig. 12: Colocalization of TGFβ ligands and decorin in WT and *Twist1*$^{+/-}$ coronal sutures at PN3.5.

Immunofluorescence co-staining of TGFβ1, TGFβ2, and TGFβ3 with decorin in WT (a-l) and *Twist1*$^{+/-}$ (m-x) coronal sutures at PN3.5. White dashed lines outline the bone edges. High magnification views of the magenta boxed regions (dural area) in d, h, l, p, t, and x are shown in d', h', l', p', t', and x', respectively. High magnification views of the yellow boxed regions (suture midline) in d, h, l, p, t, and x are shown in d'', h'', l'', p'', t'', and x'', respectively. Yellow

192 arrowheads indicate regions of TGFβ-decorin colocalization. Asterisks indicate the absence of co-
193 expression. fb, frontal bone; pb, parietal bone. Scale bars: 100 μm in a (a-x) and d (all other panels).

194

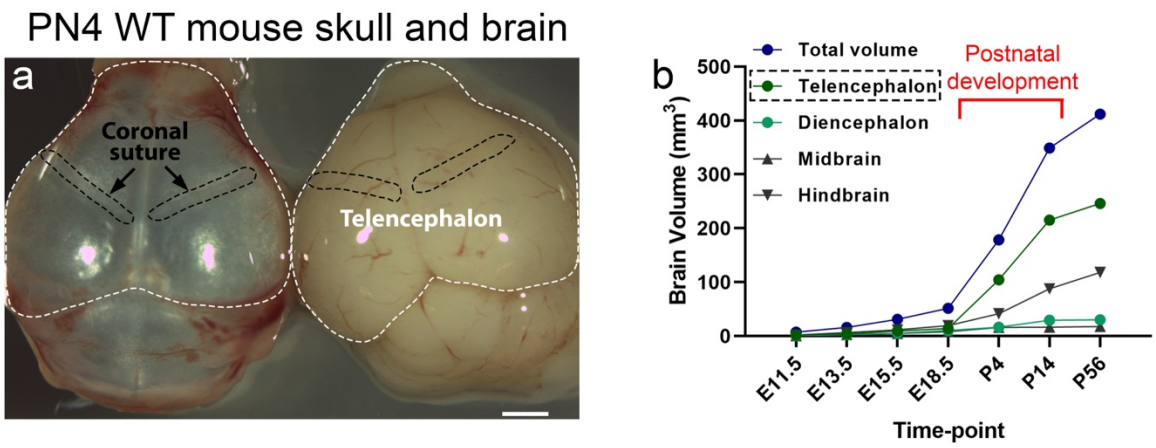

195

196 **Supplementary Fig. 13: The coronal suture is anatomically associated with the telencephalon,**

197 **which undergoes rapid expansion during postnatal development.**

198 (a) Brightfield image indicating the anatomical location of the coronal suture (black dashed line),

199 situated directly above the telencephalon (white dashed line). Scale bar: 1 mm.

200 (b) Volumes of different brain regions at various developmental stages.